BMC Neurology

RESEARCH

Open Access

Morphological vessel analysis of intracranial basal ganglia hemorrhage on computed tomography angiography image

Chang Ki Jang[1], Kwang-Chun Cho[1], Nak-Hoon Son[2], Jun-Hwee Kim[3*†] and Jiwoong Oh[4*†]

Abstract

Purpose Hypertensive intracerebral hemorrhage (ICH) of the basal ganglia mostly occurs unilaterally. Therefore, we describe the differences between the morphological parameters of lesional and non-lesional carotid arteries using initial computed tomography angiography.

Methods A total of 284 patients were diagnosed with nontraumatic ICH between March 2020 and October 2024. Hypertensive basal ganglia hemorrhages were included with a total of 64 patients enrolled in this study. Using an IntelliSpace portal, morphological examination was conducted on both the intracranial and extracranial segments on each side of the carotid artery (intra- and extra group). The total length, short distance, maximal diameter, and minimal diameter of each segment was calculated.

Results In both the intra- and extra-groups, the measured variables (Tortuosity, short distance, length, Dmin, Dmax) demonstrated no statistically significant differences between the ICH and non-ICH sides. There were no statistically significant differences in the five measured parameters after adjusting for the bleeding side to compensate for left/right (Lt/Rt) anatomical differences. To evaluate age-related alterations in blood vessels, we categorized individuals into 2 groups: those aged $\geq$65 and $\leq$65 years, ensuring a comparable distribution across the groups. Subsequently, we analyzed morphological alterations in the blood vessels of both groups. Significant differences in tortuosity and short distances within the Intra group were observed using paired *t*-tests. (tortuosity- $p=0.011$, short distance- $p=0.041$)

Conclusions Morphological analysis revealed that the bilateral carotid arteries did not differ between the intracranial and extracranial segments. However, some parameters (tortuosity and short distance) exhibited morphological changes associated with aging.

Keywords Intracerebral hemorrhage, Basal ganglia, Computed tomography angiography

†Jun-Hwee Kim and Jiwoong Oh contributed equally to this work.

*Correspondence:
Jun-Hwee Kim
kastanie83@yuhs.ac
Jiwoong Oh
worldcapture@hanmail.net

[1]Department of Neurosurgery, Yongin Severance Hospital, Yonsei University College of Medicine, Yongin, Gyeonggi-do, Republic of Korea
[2]Department of Statistics, Keimyung University, Daegu, Republic of Korea
[3]Departments of Radiology, Yongin Severance Hospital, Yonsei University College of Medicine, 363 Dongbaekjukjeondaero, Jung-dong, Giheung-gu, Yongin, Gyeonggi-do, Republic of Korea
[4]Department of Neurosurgery, Yonsei University College of Medicine, 50 Yonsei-ro,Seodaemun-gu, Seoul 120-752, South Korea

Introduction

Hemorrhagic strokes account for 10–20% of all strokes [1]. Among hemorrhagic strokes, hypertensive intracerebral hemorrhage (H-ICH) is the most common type [2]. Of the H-ICH subtypes, basal ganglia (BG) hemorrhage are the most commonly occurring lesions. BG hemorrhages are related to ruptures in the lenticulostriate artery branches, which usually originate from the middle cerebral arteries and sometimes the anterior cerebral arteries. The perforating vessels's tear is known as Charcot–Bouchard aneurysm, which refers to microaneurysms that are <0.3 mm [3]. BG intracerebral hemorrhage (BG ICH) usually shows unilateral presentation. Bilateral BG ICH is an extremely rare condition that is mainly caused by trauma [4].

The incidence of any stroke, including ischemic and hemorrhagic strokes, increases with age [5, 6]. Given that comorbidities, such as hypertension and diabetes, also worsen with age, those can account for variabilities among patients. However, in a single patient with a uniform disease state, the side of the carotid artery that is affected can be attributed to other factors. Additionally, blood vessels undergo morphological changes with aging. Accordingly, we hypothesized that age-related morphological changes can influence the carotid artery side—left or right—that is more likely to be associated with a hemorrhagic stroke incidence. Therefore, we used bilateral carotid parameters in one patient to nullify the effect of inter-patient variability in factors such as comorbidities and difference in blood pressure control status. Therefore, by comparing the carotid artery parameters of each side, the factors associated with the occurrence of BG ICH can be predicted, while excluding other factors that may influence the rupture of microvessels, such as hypertension, diabetes, and dyslipidemia.

Methods

We retrospectively collected data from 284 patients admitted with a diagnosis of spontaneous intacerebral hemorrhage between 2020 and 2024. Among these patients, those with ICH in the BG and other locations and with mixed-type ICH were excluded ($n = 167$). Among the patients with BG ICH, those with preexisting vessel abnormalities, such as Moyamoya disease, arteriovenous malformation, main vessel steno-occlusive lesions, and severe distortion of the main vessel caused by hematoma compression, were excluded ($n = 24$). Additionally, we excluded external institution CTA images, scans lacking extracranial carotid coverage, and cases where image quality—following processing with the IntelliSpace Portal—was deemed suboptimal for accurate assessment due to severe calcification or artifacts ($n = 29$). Finally, 64 patients were enrolled as eligible for this study.

Parameters

Patients' comorbidities (past history) were not included. We compared the bilateral carotid condition with the vascular parameters. Therefore, the internal conditions of the bilateral carotid arteries were the same. The collected patient parameters included sex, age, side of hemorrhage (Lt/Rt), and height. The patient height was obtained to adjust for individual differences in blood vessel length. Vascular parameters were the total length of the vessel (length)—defined as the actual path length of the segment vessel, short distance in three-dimensional space (short distance), and tortuosity value—ratio of the first two parameters [7]. The diameter was automatically measured by the IntelliSpace Portal software (Version 12.1, Philips Healthcare, Best, Netherlands) using the following method: calculating the square root of the vessel internal area divided by pi (π) and subsequently doubling it. Additionally, the minimum diameter (Dmin), which was the narrowest part of the segmental vessel, and the maximum diameter (Dmax), which was the most dilated part of the segment, were measured.

Image analysis

CT angiography was performed using a multidetector CT scanner (Philips Brilliance iCT; Philips Healthcare). For non-contrast and post-contrast brain CT, images were acquired at 120 kVp and 200 mAs, whereas the angiographic phase was obtained at 100 kVp and 160 mAs. Scan coverage included the entire brain for the pre- and post-contrast phases, and extended from the brain to the neck down to the level of the carina during the angiographic phase.

Collimation was set to 16×0.625 mm for the pre- and post-contrast phases and to an automated configuration (default 128×0.625 mm) for the angiographic phase. Image reconstruction was performed with a standard brain kernel (Brain Standard 0.0). Slice thickness and interval were 1.25 mm/1.25 mm for pre- and post-contrast images, and 0.67 mm/0.67 mm (axial) and 1.0 mm/1.0 mm (coronal) for the angiographic phase.

A nonionic iodinated contrast agent (Pamiray 370, 100 mL) was administered at an injection rate of 4 mL/s. Bolus tracking was performed with a threshold of 120 HU using a region of interest placed in the aortic arch, followed by a post-injection delay of 10 s and a scan delay of 3.4 s. Imaging was obtained in three phases: pre-contrast, angiographic, and post-contrast phases.

The enrolled patients' CTA data were post-processed using the Intellispace Portal. Vessel extraction from the entire carotid artery (from the orifice of the aorta to the distal anterior and middle cerebral arteries) was automatically performed using advanced vessel analysis sub-analysis (Fig. 1). Using the extracted carotid artery, we manually divided it into two parts: extracranial and

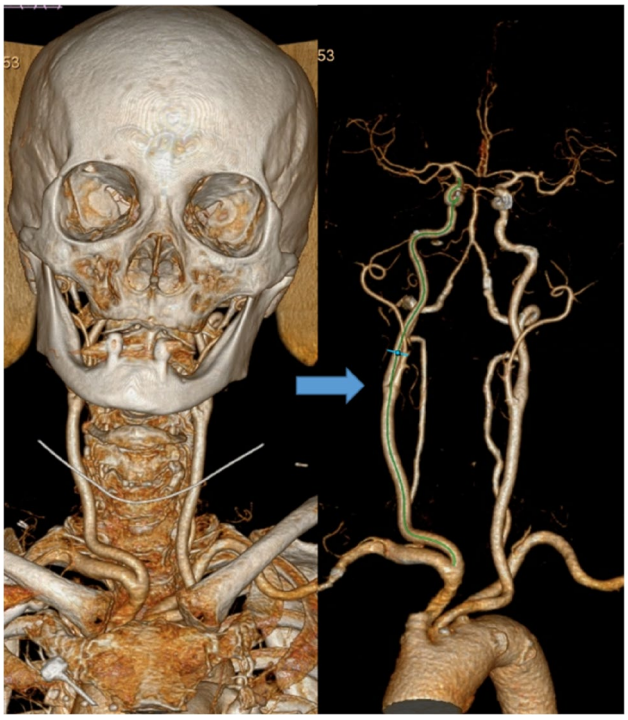

Fig. 1 Vessel extraction created for the entire carotid artery (From orifice of aorta to distal anterior and middle cerebral artery) was done automatically using advance vessel analysis sub-analysis

intracranial internal carotid artery (Extra ICA and Intra ICA). The Extra ICA was defined from the orifice of the aorta to the portion that penetrates the petrous bone (Fig. 2). The ICA was defined as the segment extending from the petrosal bone to the internal carotid artery bifurcation (ICBIF) (Fig. 3). During segmentation, we manually corrected the centerline and outer artery line for proper analysis. After complete segmentation, automatic vessel parameter analysis was performed using the software (Fig. 4).

Statistical analysis

Patient demographic variables are presented as mean± standard deviations (SD) for continuous variables and as frequencies and percentages for categorical variables. To confirm the statistical assumptions, normality tests (Shapiro–Wilk test) were performed for continuous variables. Statistical significance was set at a 5% significance level ($p< 0.05$).

Initially, we assessed the statistical significance of the parameter differences between the extra- and intra-groups. Considering that the vascular anatomy between the Rt and Lt sides differed significantly from the aortic orifice to the carotid bifurcation, an anatomical variation that may influence the hemodynamics and

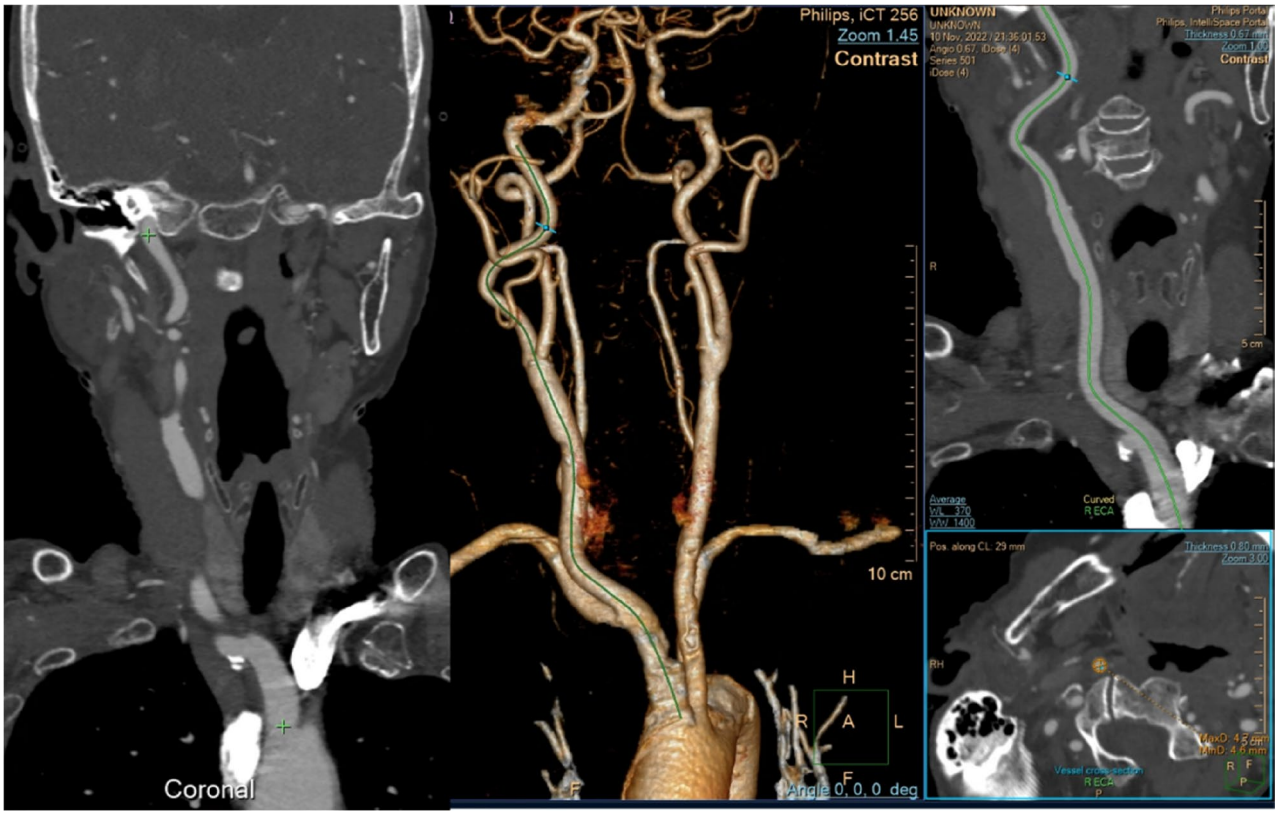

Fig. 2 The extracranial internal carotid artery is defined from the orifice of the aorta to the portion that penetrates the petrous bone. Centerline (green line) was automatically generated

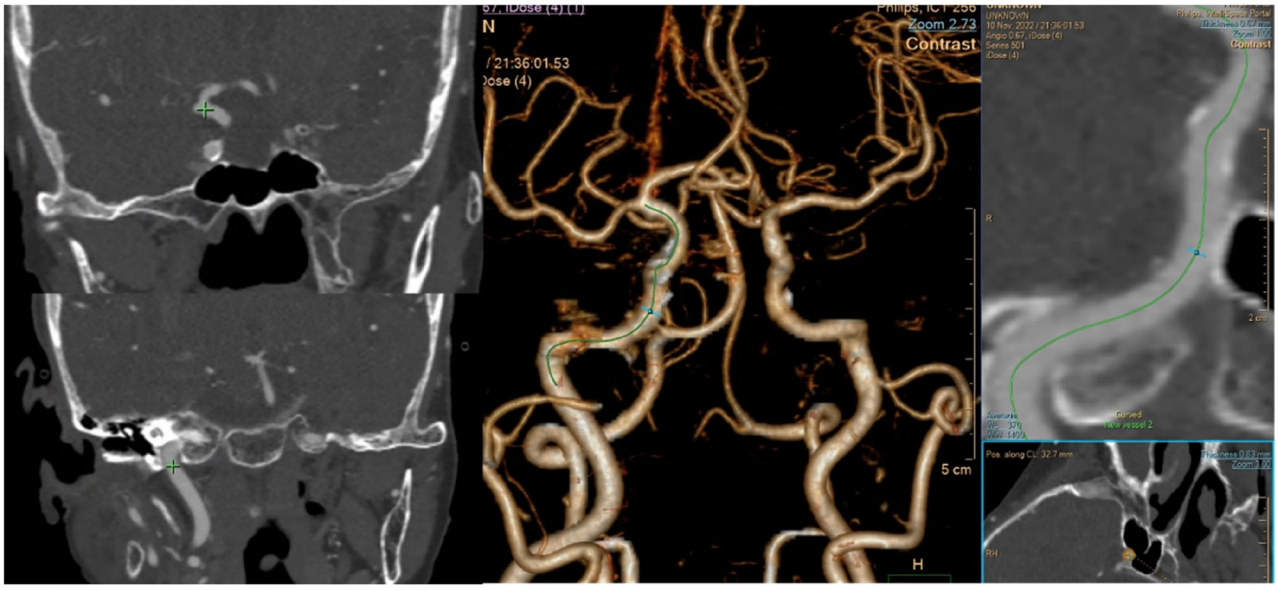

Fig. 3 The intracranial internal carotid artery is defined as the segment form the area entering the petrosal bone to the internal carotid artery bifurcation (ICBIF)

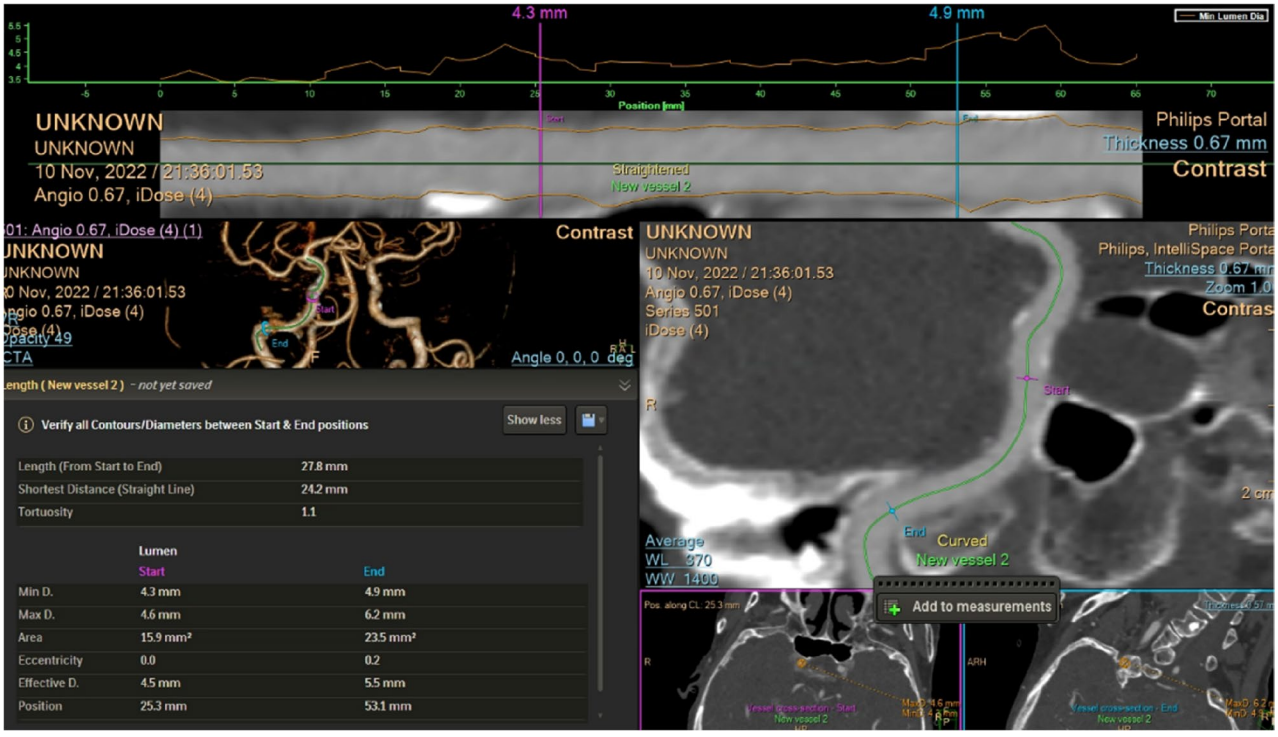

Fig. 4 During the segmentation, we manually performed the correction work for the centerline and artery outer line for proper analysis. After complete segmentation, automatically vessel parameter analysis was done using software. The automatically measured values can be reviewed immediately

pathophysiology of ICH, a mixed-effects model was applied. This approach allowed us to simultaneously analyze both the affected and contralateral hemispheres within the same patient by treating the data as repeated measurements. Furthermore, a repeated-measures design was independently applied to the intra- and extra-groups, facilitating a stepwise statistical approach for robust inference.

To properly account for interhemispheric anatomical differences, the hemorrhage-side (binary: 1 = ICH side, 0 = non-ICH side) was modeled as the dependent variable. Fixed effects were used for variables such as

height, age, and sex, which were measured in the same patient and assumed constant across observations. Contrastingly, variables representing the ICH-affected side versus the control side were modeled as repeated measures. The random-effects component was incorporated by parameterizing the covariance structure for random components associated with repeated measurements within individual patients, specifically using a random intercept for each subject (u_i) to encode within-subject pairing. The model is expressed as: $\text{logit}\left(P\left(Y_{ij}=1\right)\right)=\beta_0+X_{ij}\beta+u_i+\epsilon_{ij}$, where Y_{ij} is the outcome for side j of patient i, and X_{ij} represents the morphological predictors. Continuous predictors were standardized (z-scores) before analysis to facilitate comparison.

The mixed-effects model framework, implemented using the GLIMMIX procedure in SAS, effectively addressed both fixed and random effects, enhancing the precision and robustness of the statistical inferences. As this study was designed as an exploratory, hypothesis-generating investigation of multiple morphological parameters, no formal multiplicity adjustments (e.g., Bonferroni correction) were applied to the P-values to minimize the risk of Type II errors. Subgroup analyses were performed based on age (cutoff of 65 years) to investigate age-related changes in vascular morphology. All statistical analyses were conducted using SAS (version 9.4; SAS Institute, Cary, North Carolina, USA) and R software (version 4.2.2; R Project for Statistical Computing, Vienna, Austria).

Results

We analyzed data from 64 patients. (21 female and 43 male patients; mean age, 62 years; SD, 14.94; range, 31–91 years). The baseline characteristics of the patients with respect to the measured parameters are reported in Table 1. To account for the differences in the vascular structure between the Rt and Lt sides originating from the aorta in Table 1, we have categorized and organized the data into separate Tables.

In both the intra- and extra-groups, the measured variables (Tortuosity, Short distance, length, Dmin, Dmax) demonstrated no statistically significant differences between the ICH and non-ICH sides (Table 2). Although not statistically significant, a trend towards higher tortuosity was observed in the intra-axial group. (OR 2.63, 95% CI 0.41–16.64, $p=0.29$) The remaining parameters demonstrated minimal association, with odds ratios (ORs) approximating 1.

Table 1 Measured vascular parameters

***N*=64**	**ICH**		**Non-ICH**	
	mean or *N*	**(SD) or %**	**mean**	**(SD)**
Lt				
Intra				
Tortuosity	1.78	(0.15)	1.74	(0.16)
Short distance	44.73	(3.52)	44.64	(3.55)
Length	79.78	(8.14)	77.56	(8.06)
Dmin	3.07	(0.37)	3.15	(0.49)
Dmax	5.32	(0.65)	5.22	(0.67)
Extra				
Tortuosity	1.18	(0.06)	1.20	(0.07)
Short distance	183.81	(16.49)	188.71	(17.89)
Length	215.77	(14.65)	227.60	(17.27)
Dmin	3.74	(0.74)	3.59	(0.46)
Dmax	9.19	(1.38)	12.01	(2.91)
Rt				
Intra				
Tortuosity	1.87	(0.26)	1.83	(0.2)
Short distance	43.75	(2.68)	44.06	(3.19)
Length	81.60	(9.35)	80.48	(8.32)
Dmin	3.08	(0.43)	3.11	(0.49)
Dmax	5.05	(0.57)	5.18	(0.59)
Extra				
Tortuosity	1.22	(0.11)	1.19	(0.11)
Short distance	190.94	(18.47)	185.75	(18.13)
Length	231.20	(21.25)	219.04	(18.84)
Dmin	3.64	(0.72)	3.73	(0.6)
Dmax	12.73	(2.52)	9.40	(1.62)

Table 2 Risk factors for ICH in Intra and Extra subgroups

	ICH (ref: Non-ICH)		
	OR	**95% CI**	***P*-value**
Intra			
Tortuosity	2.632	(0.422, 16.413)	0.2945
Short distance	0.989	(0.883, 1.107)	0.8408
Length	1.023	(0.98, 1.068)	0.3008
Dmin	0.742	(0.327, 1.683)	0.4686
Dmax	0.943	(0.526, 1.69)	0.8405
Extra			
Tortuosity	1.449	(0.031, 68.144)	0.8480
Short distance	1.001	(0.981, 1.022)	0.8841
Length	1.003	(0.984, 1.022)	0.7855
Dmin	1.050	(0.594, 1.855)	0.8650
Dmax	1.066	(0.929, 1.223)	0.3561

Table 3 Risk factor analysis adjusted for hemorrhagic side (Lt or Rt)

	ICH (ref: Non-ICH)		
	OR	**95% CI**	***P*-value**
Intra			
Tortuosity	2.639	(0.419, 16.642)	0.2959
Short distance	0.990	(0.884, 1.109)	0.8614
Length	1.023	(0.98, 1.069)	0.2907
Dmin	0.735	(0.323, 1.673)	0.4566
Dmax	0.964	(0.535, 1.737)	0.9018
Extra			
Tortuosity	1.173	(0.024, 58.293)	0.9350
Short distance	1.000	(0.024, 58.293)	0.9646
Length	1.000	(0.981, 1.021)	0.9606
Dmin	1.071	(0.603, 1.9)	0.8125
Dmax	1.055	(0.892, 1.247)	0.5269

To control potential confounding effects arising from inherent anatomical differences between the Lt and Rt sides of the carotid artery, risk factor analysis was adjusted for the hemorrhagic side (Lt/Rt) (Table 3). Differences among the five measured parameters for either sides were not significant.

To evaluate age-related alterations in blood vessels, we categorized individuals into 2 groups: those aged ≥65 and<65 years, ensuring a comparable distribution across the groups. Subsequently, we analyzed morphological alterations in the blood vessels of both groups. Significant differences in tortuosity and short distances within the intra-group were observed using paired *t*-tests. (tortuosity, $p = 0.011$; short distance, $p = 0.041$) (Table 4).

Results from comparing parameters between the ICH and non-ICH groups stratified by age indicated that, within the intra-group, tortuosity was approximately 0.11 units greater in patients aged ≥ 65 years, while short distance was 1.88 units lower in the same age cohort (Table 5).

Discussion

In our study, no significant differences were observed in the parameters between the ipsilateral (ICH side) and contralateral (non-ICH side) within the intra- and extra-groups. The analysis adjusted for anatomical differences in the origin of the left and right vessels did not reveal any significant differences. Although we were unable to demonstrate statistically significant side-to-side differences, this finding suggests that unilateral intracerebral hemorrhage cannot be adequately explained by a single isolated factor. Rather, it supports the notion that additional contributors may also play important roles. However, when the cohort was stratified by age with a cutoff of 65 years, the comparison of the ICH and non-ICH groups within the older stratum (≥ 65 years) yielded distinct findings. Tortuosity in the ICH group was 0.11 units greater than that in the non-ICH group. Furthermore, short distance on the ICH side among individuals aged ≥65 years was 1.88 units lower than that in the non-ICH group. These results suggest that age-related vascular changes contribute to the risk of ICH.

Table 4 Comparison of parameters by Age Group (≥65 vs. <65)

		Age < 65 (*n* = 37)			Age ≥ 65 (*n* = 27)			independent t-test
		n	**mean**	**SD**	***n***	**mean**	**SD**	***p*-value**
Intra								
Tortuosity	ICH	35	1.82	0.16	27	1.837	0.28	0.8524
	Non- ICH	35	1.83	0.17	26	1.738	0.18	0.0510
	paired t-test p-value		0.840			0.011		
Short distance	ICH	35	45.20	2.832	27	42.92	3.03	0.0035
	Non- ICH	35	44.56	3.474	26	44.01	3.20	0.5288
	paired t-test p-value		0.279			0.041		
Length	ICH	35	82.47	7.78	27	78.50	9.61	0.0773
	Non- ICH	35	81.36	7.06	26	76.14	8.93	0.0134
	paired t-test p-value		0.218			0.098		
Dmin	ICH	35	3.01	0.40	27	3.14	0.39	0.2169
	Non- ICH	35	3.11	0.47	26	3.15	0.51	0.7979
	paired t-test p-value		0.186			0.876		
Dmax	ICH	35	5.05	0.53	27	5.33	0.69	0.0803
	Non- ICH	35	5.08	0.65	26	5.35	0.55	0.0935
	paired t-test p-value		0.808			0.972		
Extra								
Tortuosity	ICH	35	1.18	0.09	27	1.21	0.09	0.2798
	Non- ICH	35	1.17	0.08	27	1.22	0.10	0.0607
	paired t-test p-value		0.353			0.626		
Short distance	ICH	35	190.18	18.361	27	184.25	16.77	0.1951
	Non- ICH	35	188.79	18.075	27	184.99	17.86	0.4128
	paired t-test p-value		0.406			0.675		
Length	ICH	35	224.57	19.92	27	223.20	20.19	0.7910
	Non- ICH	35	221.74	19.11	27	224.73	17.84	0.5325
	paired t-test p-value		0.389			0.625		
Dmin	ICH	35	3.63	0.52	27	3.75	0.92	0.5671
	Non- ICH	35	3.54	0.33	27	3.82	0.69	0.0616
	paired t-test p-value		0.325			0.583		
Dmax	ICH	35	11.31	2.79	27	10.75	2.63	0.4296
	Non- ICH	35	10.34	3.03	27	10.98	2.03	0.3204
	paired t-test p-value		0.181			0.755		

Spontaneous ICH accounts for 10–15% of stroke with BG ICH being the most common among the ICH subtypes. Moreover, it can cause injury to the posterior limb of the internal capsule, leading to paralysis and significant disability. Charcot-Bouchard aneurysm is a microaneurysm in the brain that occurs in penetrating vessels that are <300 micrometers in diameter. The lenticulostriatal artery (LSA) is the most common artery. The rupture of these aneurysm is the main cause for ICH [8]. Similar to the spontaneous subarachnoid hemorrhage that occurs due to aneurysms, ICH is also associated with the rupture of an aneurysm. The medial LSA branches from the anterior cerebral artery are the main feeders of the inferomedial part of the head of the caudate nucleus, anterior limb of the internal capsule, and anterior and inferior regions of the putamen and globus pallidus. The lateral LSA branches from the middle cerebral artery supplies to the superolateral part of the head and body of the caudate nucleus, superior part of the entire internal capsule, most of the putamen, and part of the globus pallidus. Finally,

Table 5 Comparison of parameter difference (ICH-Non ICH) by Age Group (≥ 65 vs. <65)

	Age ≥ 65 (ref: Age < 65)		
	Estimate	**SE**	***P*-value**
Intra			
Tortuosity Difference	0.110	0.046	0.0213
Short distance Difference	-1.882	0.840	0.0288
Length Difference	1.123	1.521	0.4631
Dmin Difference	0.112	0.107	0.3017
Dmax Difference	0.025	0.166	0.8822
Extra			
Tortuosity Difference	-0.019	0.019	0.3282
Short distance Difference	-2.138	2.439	0.3842
Length Difference	-4.354	4.582	0.3458
Dmin Difference	-0.166	0.157	0.2954
Dmax Difference	-1.201	1.034	0.2498

the anterior choroidal branches provide flow to the medial segment of the globus pallidus, the inferior part of the posterior limb, and the retrolenticular and sublenticular portions of the internal capsule [9]. We concluded that the morphological aspects of the artery from the carotid orifice to the ICBIF can affect blood supply to the BG. Therefore, this study defines this segment as the focus of analysis. However, no significant correlation was found between ICH and the vessel parameters.

With age, the risk of stroke, including hemorrhagic stroke, gradually increases and is influenced by various factors [5]. Among which the occurrence of diseases such as hypertension and diabetes plays a major role [10]. Additionally, vascular aging is a significant factor. it is attributed to histological and structural changes in blood vessels [11]. The changes in endothelial cells and smooth muscle cells in vessels induced by oxidative stress and inflammatory response that progress with aging. Vascular aging can cause diseases such as hypertension and atherosclerosis, and can also exacerbate these diseases [12]. These changes are observed not only in histological alterations but also in morphological aspects such as tortuosity and stenosis. Sun et al. reported that definite age-related changes were observed in the neck artery, with these changes being more pronounced in women [13].

Although there is no clear evidence directly linking Charcot–Bouchard aneurysms to specific vascular morphological parameters, some reports have suggested a correlation between intracranial aneurysms and morphological parameters. Their morphological characteristics suggest a pathophysiological mechanism similar to cerebral aneurysms. Therefore, we explored the relationship between vascular morphological parameters and cerebral aneurysms as a proxy for understanding the possible associations. First, aneurysm occurrence is associated with the tortuosity index, particularly in outer curvature aneurysms. The bifurcation type with a low TI score had an increased recanalization rate [14]. Another study reported a linked between increased vascular tortuosity and aneurysm formation, although it is less likely to be connected with the physical characteristics of the ruptured aneurysms, such as a bigger maximal diameter and higher SR [15]. Roger et al. reported that reduced tortuosity may mitigate the risk of internal carotid artery aneurysm rupture and poor subarachnoid hemorrhage outcome. Internal carotid artery aneurysm growth is associated with greater tortuosity [16]. Hence aneurysm formation and growth are closely related to tortuosity. Second, stenosis is associated with aneurysms. Using CFD analysis, Kono et al. revealed that proximal stenosis may result in de novo aneurysm formation by producing high WSS and high positive WSSG at the apex [17]. Another CFD study showed that the degree of proximal M1 stenosis and its proximity to the aneurysm neck are related to the ruptured status in middle cerebral artery bifurcation aneurysms [18].

This study has some limitations. First, given the relatively modest sample size ($n = 64$), our findings should be interpreted as exploratory and hypothesis-generating. While macroscopic carotid parameters did not show significant differences in the primary analysis, this may be due to the limited statistical power to detect very subtle morphological changes. However, the use of internal controls and mixed-effects modeling maximized statistical efficiency by eliminating inter-individual confounding. Second, the age cutoff of 65 years was employed based on clinical definitions of vascular aging, but we acknowledge that dichotomizing continuous variables can lead to a loss of statistical information. Our age-stratified analysis in Table 5 reveals that certain morphological alterations, such as tortuosity ($P = 0.0213$), may emerge as significant factors in older populations. Future studies incorporating automated analysis systems and larger multi-center datasets are essential to validate these preliminary findings and.

Conclusion

Morphological analysis revealed that the bilateral carotid arteries did not differ between the Extra ICA and Intra ICA segments. However, some parameters (tortuosity and short distance) exhibited morphological changes associated with aging.

Acknowledgements
This study was supported by a faculty research grant from Yonsei University College of Medicine (6-2024-0115).

Authors' contributions
All authors contributed to the study conception and design. Writing - original draft preparation: CKJ ; Conceptualization: CKJ, KCC, JHK, JO; Methodology: CKJ, JHK; Formal analysis and investigation: NHS. Final approval of the version to be published. Agree to be accountable for all aspects of the work in ensuring that questions related to the accuracy or integrity of any part of the work are appropriately investigated and resolved: CKJ, KCC, NHS, JHK, JO.

Funding
No funding was received for this study.

Data availability
The datasets generated and/or analyzed during the current study are available from the corresponding author on reasonable request.

Declarations

Ethics approval and consent to participate
The data analysis and this study were approved by the Institutional Research Ethics Committee of the Yongin Severance hospital in Yonsei university (9-2025-0230). All procedures performed in the studies involving human participants were in accordance with the ethical standards of our Institutional Review Board with the 1964 Helsinki Declaration and its later amendments or comparable ethical standards. The requirement for informed consent was waived owing to the retrospective design of the study and the use of de-identified data.

Consent for publication
Not applicable.

Competing interests
The authors declare no competing interests.

Received: 16 December 2025 / Accepted: 6 March 2026
Published online: 17 March 2026

References

1. Sacco S, Marini C, Toni D, Olivieri L, Carolei A. Incidence and 10-year survival of intracerebral hemorrhage in a population-based registry. Stroke. 2009;40(2):394–9. https://doi.org/10.1161/STROKEAHA.108.523209.
2. Meretoja A, Strbian D, Putaala J, Curtze S, Haapaniemi E, Mustanoja S, Sairanen T, Satopaa J, Silvennoinen H, Niemela M, Kaste M, Tatlisumak T. Smash-u: A proposal for etiologic classification of intracerebral hemorrhage. Stroke. 2012;43(10):2592–7. https://doi.org/10.1161/STROKEAHA.112.661603.
3. Akmal S, Jumah F, Ginalis EE, Raju B, Nanda A. Charles jacques bouchard (1837–1915) and the charcot-bouchard aneurysm. J Neurosurg. 2022;136(5):1470–4. https://doi.org/10.3171/2021.4.JNS21583.
4. Watanabe G, Conching A, Ogasawara C, Chavda V, Bin-Alamer O, Haider AS, Priola SM, Sharma M, Hoz SS, Chaurasia B, Umana GE, Palmisciano P. Bilateral basal ganglia hemorrhage: A systematic review of etiologies, management strategies, and clinical outcomes. Neurosurg Rev. 2023;46(1):135. https://doi.org/10.1007/s10143-023-02044-x.
5. Wang S, Zou XL, Wu LX, Zhou HF, Xiao L, Yao T, Zhang Y, Ma J, Zeng Y, Zhang L. Epidemiology of intracerebral hemorrhage: A systematic review and meta-analysis. Front Neurol. 2022;13:915813. https://doi.org/10.3389/fneur.2022.915813.
6. Chen RL, Balami JS, Esiri MM, Chen LK, Buchan AM. Ischemic stroke in the elderly: An overview of evidence. Nat Rev Neurol. 2010;6(5):256–65. https://doi.org/10.1038/nrneurol.2010.36.
7. Han HC. Twisted blood vessels: Symptoms, etiology and biomechanical mechanisms. J Vasc Res. 2012;49(3):185–97. https://doi.org/10.1159/000335123.
8. Horn EM, Zabramski JM, Feiz-Erfan I, Lanzino G, McDougall CG. Distal lenticulostriate artery aneurysm rupture presenting as intraparenchymal hemorrhage: Case report. Neurosurgery. 2004;55(3):708. https://doi.org/10.1227/01.neu.0000134561.59093.d7.
9. Djulejic V, Marinkovic S, Georgievski B, Stijak L, Aksic M, Puskas L, Milic I. Clinical significance of blood supply to the internal capsule and basal ganglia. J Clin Neurosci. 2016;25:19–26. https://doi.org/10.1016/j.jocn.2015.04.034.
10. Kleindorfer DO, Towfighi A, Chaturvedi S, Cockroft KM, Gutierrez J, Lombardi-Hill D, Kamel H, Kernan WN, Kittner SJ, Leira EC, Lennon O, Meschia JF, Nguyen TN, Pollak PM, Santangeli P, Sharrief AZ, Smith SC Jr., Turan TN, Williams LS. 2021 guideline for the prevention of stroke in patients with stroke and transient ischemic attack: A guideline from the american heart association/american stroke association. Stroke. 2021;52(7):e364–467. https://doi.org/10.1161/STR.0000000000000375.
11. Liu L, Zhao B, Yu Y, Gao W, Liu W, Chen L, Xia Z, Cao Q. Vascular aging in ischemic stroke. J Am Heart Assoc. 2024;13(15):e033341. https://doi.org/10.1161/JAHA.123.033341.
12. Mistriotis P, Andreadis ST. Vascular aging: Molecular mechanisms and potential treatments for vascular rejuvenation. Ageing Res Rev. 2017;37:94–116. https://doi.org/10.1016/j.arr.2017.05.006.
13. Sun Z, Jiang D, Liu P, Muccio M, Li C, Cao Y, Wisniewski TM, Lu H, Ge Y. Age-related tortuosity of carotid and vertebral arteries: Quantitative evaluation with mr angiography. Front Neurol. 2022;13:858805. https://doi.org/10.3389/fneur.2022.858805.
14. Kim HJ, Song HN, Lee JE, Kim YC, Baek IY, Kim YS, Chung JW, Jee TK, Yeon JY, Bang OY, Kim GM, Kim KH, Kim JS, Hong SC, Seo WK, Jeon P. How cerebral vessel tortuosity affects development and recurrence of aneurysm: Outer curvature versus bifurcation type. J Stroke. 2021;23(2):213–. https://doi.org/10.5853/jos.2020.04399.
15. Li R, Zhou P, Kao E, Zhu C, Mossa-Basha M, Wang Y. Unilateral cerebral arterial tortuosity: Associated with aneurysm occurrence, but potentially inversely associated with aneurysm rupture. Eur J Radiol. 2023;165:110941. https://doi.org/10.1016/j.ejrad.2023.110941.
16. Krzyzewski RM, Klis KM, Kwinta BM, Lasocha B, Brzegowy P, Popiela TJ, Gasowski J. Subarachnoid hemorrhage from ruptured internal carotid artery aneurysm: Association with arterial tortuosity. World Neurosurg. 2022;166:e84–92. https://doi.org/10.1016/j.wneu.2022.06.101.
17. Kono K, Masuo O, Nakao N, Meng H. De novo cerebral aneurysm formation associated with proximal stenosis. Neurosurgery. 2013;73(6):E1080–1090. https://doi.org/10.1227/NEU.0000000000000065.
18. Antonov A, Kono K, Greim-Kuczewski K, Hippelheuser JE, Lauric A, Malek AM. Proximal stenosis is associated with rupture status in middle cerebral artery aneurysms. World Neurosurg. 2018;109:E835–44. https://doi.org/10.1016/j.wneu.2017.10.108.

Publisher's Note